



SPE 99288

Generalized Analytical Solution for Reservoir Problems With Multiple Wells and Boundary Conditions

G. Buswell, SPE, R. Banerjee, SPE, R.K.M. Thambynayagam, SPE, and J. Spath, SPE, Schlumberger Oilfield Services

Copyright 2006, Society of Petroleum Engineers

This paper was prepared for presentation at the 2006 SPE Intelligent Energy Conference and Exhibition held in Amsterdam, The Netherlands, 11–13 April 2006.

This paper was selected for presentation by an SPE Program Committee following review of information contained in an abstract submitted by the author(s). Contents of the paper, as presented, have not been reviewed by the Society of Petroleum Engineers and are subject to correction by the author(s). The material, as presented, does not necessarily reflect any position of the Society of Petroleum Engineers, its officers, or members. Papers presented at SPE meetings are subject to publication review by Editorial Committees of the Society of Petroleum Engineers. Electronic reproduction, distribution, or storage of any part of this paper for commercial purposes without the written consent of the Society of Petroleum Engineers is prohibited. Permission to reproduce in print is restricted to an abstract of not more than 300 words; illustrations may not be copied. The abstract must contain conspicuous acknowledgment of where and by whom the paper was presented. Write Librarian, SPE, P.O. Box 833836, Richardson, TX 75083-3836, U.S.A., fax 01-972-952-9435.

Abstract

We present a set of new analytical solutions to the single layer reservoir problem, both in real time and Laplace space. The solutions are derived assuming a cuboid shaped reservoir using a method of integral transforms. The method can be applied to calculate the pressure as a function of position and time when using any continuous function to describe the production rate of a point source. Successive integration of the point source solution can be performed to calculate the average bottom hole pressure of a well.

These equations are applicable to partially penetrating vertical, horizontal and fractured wells and take into account superposition effects in multi-well and multi-rate scenarios. Notably, regarding fractured wells, we are able to accurately model the case of a finite conductivity fracture with non-Darcy flow as well as those of infinite conductivity. The generality of our method allows any continuous function of position and time to be used to treat either pressures or fluid fluxes on the boundaries.

Also, using solutions in Laplace space we are able to model naturally fractured reservoirs, wellbore storage, non-Darcy D-factors as well as constant well pressure production, also all within a full field multi-well scenario. Our method, therefore, provides a powerful alternative to simulation in terms of reservoir modeling.

We present a comparison of our solutions with that generated using a commercial finite difference simulator for a variety of problems in terms of accuracy and speed. We find amazing accuracy with massive gains (factors > 300) in CPU times for fracture problems in particular.

Introduction

Reservoir simulation is an essential tool for the management of oil and gas reservoirs. Prediction of pressure-production behaviour under various operating conditions allows, among other benefits, proper investment decisions to be made. In order to make such a prediction one must construct a reservoir model. History matching observed behaviour of the reservoir must validate the parameters of this model.

Ideally, finite difference numerical simulators are used to construct reservoir models. However, in order to make full use of such a tool a large amount of reliable data is required. Also a full study, including a history-matching analysis, may take months to carry out. Therefore, there is a need for an alternative tool that honours the physics of fluid flow and at the same time offers a solution many orders quicker. Analytical solutions are fast and provide a broad understanding of the reservoir dynamics.

The equations applicable to laminar flow of fluids in a porous medium were the results of Darcy's experimental study of the flow characteristics of sand filters. This combined with the equation of continuity and an equation of state for slightly compressible fluid gives the diffusivity equation, which is the equation for pressure diffusion in porous medium.

Solution of the diffusivity equation under different boundary condition forms the basis for prediction of bottom hole pressure response of a producing well. These analytical solutions are generally applicable for a single well and used widely in the area of well testing. The efficiency of analytical models is generally judged by accuracy and speed.

The application of integral transform techniques to solve physical problems involving linear partial differential equations is well known. The theory has been extensively developed and given by Sneddon¹, Churchill^{2,3} and Tranter⁴. A common practice in solving linear partial differential equations is to use the classical Fourier methods in the space-variables after removing the time variable by Laplace transformation. The classical methods often require at their outset a correct form of the solution that satisfies the governing differential equation. Hence, with these methods, solutions are developed to provide answers to specific problems. The integral transform techniques on the other hand are direct and can be applied to a wide range of general class

of problems. Titchmarsh⁵ and Korner⁶ presented rigorous mathematical treatment of the theory of integral transforms. Thambynayagam⁷ provides practical and elegant solutions to problems in diffusion by the use of successive integral transforms. In our work we use these techniques to solve the generalized multi-well problem in single-phase hydrocarbon reservoirs. In the case of gas, the partial differential equations have been linearized by application of real gas pseudo-pressure as described by Al-Hussainy et al⁸. At low pressures linearization was improved by using Agarwal's pseudo-time⁹ along with pseudo-pressure.

Formulation of the Problem

We consider a cuboid model of a reservoir. The reservoir is penetrated by multiple wells both in the vertical and horizontal directions. The horizontal wells are parallel to any of the axes of the cuboid. The six faces of the cuboid can have either no-flow or constant pressure boundaries. The wells may be fractured or unfractured. A representation of the reservoir model is presented in Figure 1.

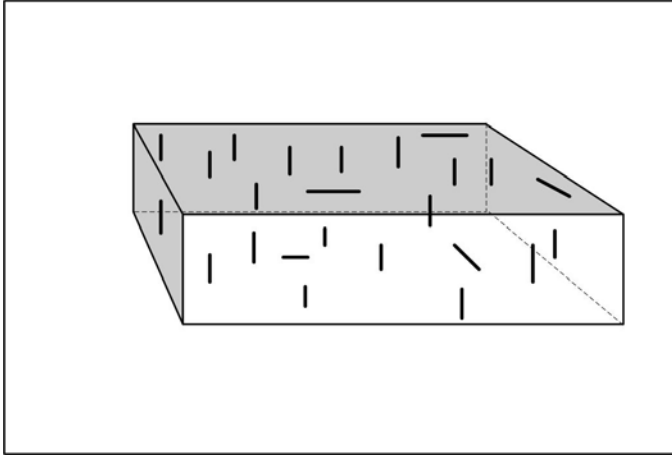


Figure 1: Cuboid reservoir with multiple completions

Our model consists of a single layer, cuboid reservoir bounded by the planes passing through $x=0$, $x=a$; $y=0$, $y=b$; $z=0$, $z=d$.

The reservoir has porosity ϕ and permeability k_x , k_y , k_z in the x , y and z directions respectively. We consider the case of a single vertical well or line source completed between the coordinates $(x_{0v}, y_{0v}, z_{01v})$ and $(x_{0v}, y_{0v}, z_{02v})$

producing fluid at rate $q(t)$ for $t > t_0$. In this particular example, the boundary conditions on each face of the homogeneous cuboid are of the Neumann type (i.e. they describe flux conditions on the boundaries) such that for $t > 0$ they satisfy the following conditions:

$$(1) \quad \frac{\partial p(0, y, z, t)}{\partial x} = - \left(\frac{\mu}{k_x} \right) \psi_{0yz}(y, z, t)$$

$$(2) \quad \frac{\partial p(a, y, z, t)}{\partial x} = - \left(\frac{\mu}{k_x} \right) \psi_{ayz}(y, z, t)$$

$$(3) \quad \frac{\partial p(x, 0, z, t)}{\partial y} = - \left(\frac{\mu}{k_y} \right) \psi_{x0z}(x, z, t)$$

$$(4) \quad \frac{\partial p(x, b, z, t)}{\partial y} = - \left(\frac{\mu}{k_y} \right) \psi_{xbz}(x, z, t)$$

$$(5) \quad \frac{\partial p(x, y, 0, t)}{\partial z} = - \left(\frac{\mu}{k_z} \right) \psi_{xy0}(x, y, t)$$

$$(6) \quad \frac{\partial p(x, y, d, t)}{\partial z} = - \left(\frac{\mu}{k_z} \right) \psi_{xyd}(x, y, t)$$

where for instance, $\psi_{0yz}(y, z, t)$ is the flux as a function of position across the (y, z) plane at $x=0$. Assuming a slightly compressible fluid with compressibility c_o , the pressure $p(x, y, z, t)$ can be shown to satisfy the diffusivity equation:

$$(7) \quad \phi c_t \frac{\partial p}{\partial t} = k_x \frac{\partial^2 p}{\partial x^2} + k_y \frac{\partial^2 p}{\partial y^2} + k_z \frac{\partial^2 p}{\partial z^2}$$

where $c_t = c_o + c_R$ and is the total compressibility of the system assuming a rock compressibility, c_R . See for example Aziz and Settari¹⁰ for a derivation of the diffusivity equation using the assumptions we have outlined.

Single Vertical Partially Penetrating Well

Using a method of integral transforms devised by Thambynayagam⁷ a solution for the average pressure of a single, vertical, partially penetrating well can be derived in the form:

$$(8) \quad p_v(x, y, t) = \frac{U(t-t_0)d}{2\pi^2 abc \phi |z_{02v} - z_{01v}|^2} \int_0^{t-t_0} q(t-t_0-\tau) \times \left\{ S_x(x, x_{0v}, \tau) S_y(y, y_{0v}, \tau) S_z^{\text{JJ}}(z_{01v}, z_{02v}, z_{01v}, z_{02v}, \tau) \right\} d\tau + \frac{4}{\phi c_t abd |z_{02v} - z_{01v}|} \int_0^t \left\{ \sum_{i=x,y,z} B_i^{\text{J}}(x, y, z_{01v}, z_{02v}, \tau) \right\} d\tau + \frac{1}{4ab\pi |z_{02v} - z_{01v}|} \times \int_0^a \int_0^b \int_0^d \phi(u, v, w) \left\{ I_x(u, x) I_y(v, y) I_z^{\text{J}}(w, z_{01v}, z_{02v}) \right\} dudvdw$$

where $\phi(x, y, z) = p(x, y, z, 0)$ and describes the initial pressure of the reservoir. We define $q < 0$ to signify producing fluid. A positive value can be used for q to signify

injection. We refer to the first term as the source term which describes the pressure contribution from the producing line source. The second term we call the boundary term since it describes the pressure contribution due to the fluid flow across the boundaries. Finally, the third term is the initial term which dictates the pressure contribution due to the initial conditions of the reservoir. The source functions,

$S_x(x, x_{0v}, \tau), S_y(y, y_{0v}, \tau), S_z^{\text{fff}}(z_{01v}, z_{02v}, z_{01v}, z_{02v}, \tau)$,
boundary

functions, $B_x^{\text{f}}(x, y, z_{01v}, z_{02v}, \tau), B_y^{\text{f}}(x, y, z_{01v}, z_{02v}, \tau),$

$B_z^{\text{f}}(x, y, z_{01v}, z_{02v}, \tau)$ and initial functions,

$I_x(u, x), I_y(v, y), I_z^{\text{f}}(w, z_{01v}, z_{02v})$ are defined in

Appendix C. A detailed description of the solution derivation of equation (8) is described in Appendix A.

The point (x, y) is chosen in equation (8) such that it is evaluated at the well radius so that our solution then describes the average pressure along the well radius. We have found that the average pressure is an excellent approximate to the bottom hole pressure (BHP) of the well and evidence of this is shown in our comparisons with the ECLIPSE* reservoir simulator.

Analytic solutions for a uniform flux well with constant sandface rate in a sealed, box-shaped reservoir have been discussed fairly extensively in the literature^{11,12,13,14}. Our method, on the other hand, fully accounts for the general description of boundary and initial conditions we have outlined.

In our example solution we have considered flux or Neumann boundary conditions on all faces of our cuboid, but this need not be the case. The Dirichlet condition:

$$(9) \quad p(0, y, z, t) = p_{0,yz}(y, z, t)$$

could be used for example to specify the pressure as a function of y, z and t on the $x=0$ boundary. An application of this kind of boundary condition would be to model the pressure support from an aquifer. A Robin condition could also specify a mixture of pressure and flux conditions in the form:

$$(10) \quad p(0, y, z, t) + \frac{\partial p(0, y, z, t)}{\partial x} = p_{0,yz}(y, z, t) - \left(\frac{\mu}{k_x}\right) \psi_{0,yz}(y, z, t)$$

The method of Thambynayagam⁷ can handle all permutations of the Neumann, Dirichlet and Robin conditions over the six

faces of the cuboid. However, in this paper we will deal with Neumann boundary conditions only.

There is clearly huge scope for practical applications of these solutions, both in single layer and multiple layer reservoir problems. The multiple layer scenario can be modeled by numerically solving for the crossflow between layers. Once one has this crossflow as a function of position and time between each pair of adjacent layers then these analytical solutions can be applied directly to calculate the pressure anywhere in the reservoir. In this paper we will focus on single layer problems.

Multiple Horizontal and Vertical Wells

Let us consider a sealed (i.e. no fluid flow across any of the boundaries) single layer reservoir. If we assume that our well produces at constant rate $q\forall t$ and that the initial pressure $p(x, y, z, 0) = p_I$ then we have a special case of equation (8) where the boundary term vanishes and the initial term is a constant, equal to p_I , so that the average pressure of a single vertical well is:

(11)

$$p_v(x, y, t) = p_I + \frac{qd}{2\pi^2 abc_i \phi |z_{02v} - z_{01v}|^2} \times \int_0^t \left\{ S_x(x, x_{0v}, \tau) S_y(y, y_{0v}, \tau) S_z^{\text{fff}}(z_{01v}, z_{02v}, z_{01v}, z_{02v}, \tau) \right\} d\tau$$

In any real reservoir problem the rate history of a well will be a function of time. In the petroleum industry an often-used condition is:

$$(12) \quad q(t) = \sum_{i=1}^M \Delta q_i U(t - t_i), \quad [t_0 < t_1 < t_2 \dots < t_{M-1}, t_M]$$

where $\Delta q_i = q_i - q_{i-1}$. One can then use the principle of superposition as outlined for example in Sabet¹⁵ which easily lends itself to our solutions. The average pressure of our single vertical well using the rate history defined in equation (12) can then be written as:

(13)

$$p_v(x, y, t) = p_I + \frac{d}{2\pi^2 abc_i \phi |z_{02v} - z_{01v}|^2} \sum_{i=0}^M \Delta q_i U(t - t_i) \times \int_0^{t-t_i} \left\{ S_x(x, x_{0v}, \tau) S_y(y, y_{0v}, \tau) S_z^{\text{fff}}(z_{01v}, z_{02v}, z_{01v}, z_{02v}, \tau) \right\} d\tau$$

Our model provides much flexibility in terms of the placement of wells in the reservoir meaning we can use our solutions to solve all manner of both well testing and full field simulation problems with multiple wells (both horizontal and vertical).

* Mark of Schlumberger

To give an example which nicely illustrates the power of these solutions let us assume we have a reservoir model consisting of a vertical and a horizontal well. The vertical well has perforation end-points at (x_v, y_v, z_{01v}) and

(x_v, y_v, z_{02v}) and the horizontal well at (x_{01h}, y_h, z_h) and (x_{02h}, y_h, z_h) . We also assume that the vertical and horizontal wells have rate history:

$$(14) \quad q_v(t) = \sum_{i=1}^M \Delta q_{vi} U(t-t_{vi}), [t_{v0} < t_{v1} < t_{v2} \dots < t_{vM-1}, t_{vM}]$$

$$(15) \quad q_h(t) = \sum_{j=1}^N \Delta q_{hj} U(t-t_{hj}), [t_{h0} < t_{h1} < t_{h2} \dots < t_{hN-1}, t_{hN}]$$

The average pressures of our vertical and horizontal wells, $p_v(x, y, t)$ and $p_h(y, z, t)$ respectively can then be written as:

$$(16) \quad p_v(x, y, t) = \frac{d}{2\pi^2 abc_t \phi |z_{02v} - z_{01v}|^2} \sum_{i=0}^M \Delta q_{vi} U(t-t_{vi}) \times \\ \times \int_0^{t-t_{vi}} \left\{ S_x^J(x_v, \tau) S_y^J(y_v, \tau) S_z^{JJ}(z_{01v}, z_{02v}, z_{01v}, z_{02v}, \tau) \right\} d\tau \\ + \frac{1}{2\pi^2 bc_t \phi |z_{02v} - z_{01v}| |x_{02h} - x_{01h}|} \sum_{j=0}^M \Delta q_{hj} U(t-t_{hj}) \times \\ \times \int_0^{t-t_{hj}} \left\{ S_x^J(x_{01h}, x_{02h}, \tau) S_y^J(y_h, \tau) S_z^J(z_{01v}, z_{02v}, \tau) \right\} d\tau + p_I$$

$$(17) \quad p_h(y, z, t) = \frac{a}{2\pi^2 bdc_t \phi |z_{02v} - z_{01v}|^2} \sum_{j=0}^N \Delta q_{hj} U(t-t_{hj}) \times \\ \times \int_0^{t-t_{hj}} \left\{ S_x^{JJ}(x_{01h}, x_{02h}, x_{01h}, x_{02h}, \tau) S_y^J(y_h, \tau) S_z^J(z_h, \tau) \right\} d\tau \\ + \frac{1}{2\pi^2 bc_t \phi |z_{02v} - z_{01v}| |x_{02h} - x_{01h}|} \sum_{i=0}^M \Delta q_{vi} U(t-t_{vi}) \times \\ \times \int_0^{t-t_{vi}} \left\{ S_x^J(x_{01h}, x_{02h}, \tau) S_y^J(y_h, \tau) S_z^J(z_{01v}, z_{02v}, \tau) \right\} d\tau + p_I$$

The point (x, y) is then chosen in equation (16) such that it is evaluated at the well radius. The same is true of the point (y, z) in equation (17). In the above expressions for the

average pressure of our vertical and horizontal wells interference effects between the wells are fully accounted for over all time regimes of interest. Clearly our method can be applied to similar problems where any number of wells are specified.

Hydraulic Fractures

We can also model fractured wells using our integral transform technique. Whereas the well is considered as a uniform flux line source, a hydraulic fracture in our model is considered as a uniform flux plane source similar to that of Gringarten et al¹⁶. The source term for the average pressure of a hydraulically fractured vertical well in the (x, z) plane producing at constant rate q can be obtained by integrating equation (11) with respect to x_0 , from x_{01} to x_{02} , to give:

$$(18) \quad p_v(x, y, t) = p_I + \frac{qd}{\pi^3 bc_t \phi |z_{02} - z_{01}|^2 |x_{02} - x_{01}|} \times \\ \times \int_0^t \left\{ S_x^J(x, x_{01}, x_{02}, \tau) + S_y^J(y, \tau) + S_z^{JJ}(z_{01}, z_{02}, z_{01}, z_{02}, \tau) \right\} d\tau$$

We assume that the vertical well completion bisects the rectangular fracture so that it is defined over the interval between the points $((x_{02} + x_{01})/2, y_v, z_{01})$ and $((x_{02} + x_{01})/2, y_v, z_{02})$ and the fracture is bounded by the planes $x = x_{01}$, $x = x_{02}$, $z = z_{01}$, $z = z_{02}$. The crucial difference between our model and that of Gringarten is that, firstly, the fracture does not have to fully penetrate the formation and secondly, we do not assume the reservoir is infinite in extent in the x and y directions. In the above example our uniform flux fracture produces at a constant rate but this can be extended to a multi-rate scenario using a similar approach that led us from equation (11) to (13).

While the so-called uniform flux model gives a good approximation to a fracture with high conductivity, in order to model fractures with low to intermediate conductivity the flow dynamics inside the fracture must be considered.

Finite Conductivity Fractures with Non-Darcy Flow

We have developed a model of a finite conductivity fracture with non-Darcy flow using our solution for rectangular sources in conjunction with a technique based on that of Guppy¹⁷ to model flow within the fracture itself. The method of solution involves forming two separate models. The first models flow from the formation into the fracture, which we will refer to as the Formation Model, The second models fluid flow inside the fracture as it flows to the well where it is produced, which we will refer to as the Fracture Model.

Formation Flow Model

The Formation Model, as has been the case throughout this paper, consists of a cuboid reservoir of length a , width b and

height d . We again consider a vertical well which bisects a rectangular vertical fracture in the (x, z) plane. The well is perforated between the points (x_v, y_v, z_{01v}) and (x_v, y_v, z_{02v}) . The fracture has half-length x_f and is bounded by the planes $x = x_v - x_f$, $x = x_v + x_f$, $z = z_{01v}$ and $z = z_{02v}$. We also split our rectangular fracture into $2N$ equal segments of length Δx , although because of symmetry we consider only half the fracture, from $x = x_v$ to $x = x_v + x_f$. The coordinates of the centre of fracture segment j are $(x_j, y_v, (z_{02v} + z_{01v})/2)$. Figure 2 illustrates the problem with a cross-section through the reservoir at the point y_v .

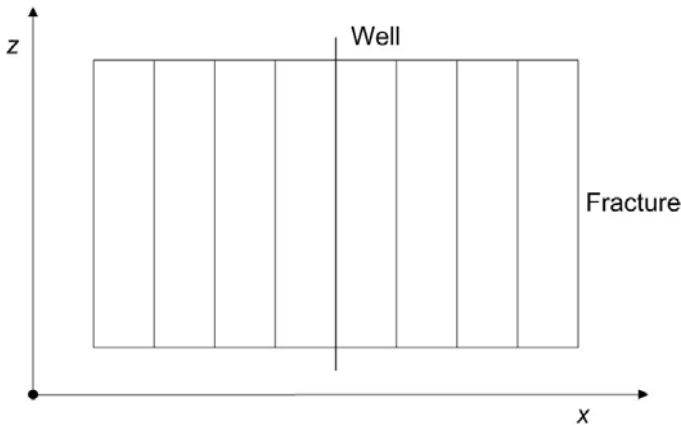


Figure 2: Fracture parallel to the x-axis split into $2N$ segments

We also assume we have M time intervals so that $[t_0 < t_1 < t_2 \dots < t_{M-1}, t_M]$. Fluid from the formation flows into the fracture and we assume that segment j produces fluid at constant rate q_{fjk} between time intervals t_k and t_{k+1} . If the fracture produces at constant rate $q \forall t$, then at any time t_k we have the constraint $\sum_{j=1}^N q_{fjk} = q/2$ for the half of the fracture we are considering. The average pressure of the surface of fracture segment j , which we denote $p_{fj}(t)$, producing at constant rate q_{fj} can then be obtained by setting the appropriate segment coordinates in equation (18) and integrating over the range of x values that the fracture segment spans. This gives us the expression:

(19)

$$p_{fj}(t) = p_I + \frac{2q_{fj}ad}{\pi^4 bc_r \phi |z_{02v} - z_{01v}|^2 \Delta x^2} \times \int_0^t \left\{ S_x^{\text{Jf}}(x_{jl}, x_{jl}, x_{ju}, x_{ju}, \tau) + S_y(y_v, \tau) + S_z^{\text{Jf}}(z_{01}, z_{02}, z_{01}, z_{02}, \tau) \right\} d\tau$$

where $x_{jl} = x_j - \Delta x/2$ and $x_{ju} = x_j + \Delta x/2$ are the lower and upper positions of fracture segment j on the x axis respectively.

However, equation (19) ignores the fact that a fracture segment will feel a pressure drop due to fluid entering other fracture segments as well as itself. We must also allow for the fact that at time, t_{k+1} the fluid production rate of segment j , q_{fjk+1} , will be different to the production at time t_k due possibly to boundary effects and flow within the fracture as a whole. We use the principle of superposition in time and space to account for these effects and obtain an expression for the average pressure over fracture segment j in the form:

(20)

$$p_{fj}(t) = p_I + \sum_{i=1}^N \sum_{k=1}^M \frac{2\Delta q_{fjk} U(t - t_k) ad}{\pi^4 bc_r \phi |z_{02v} - z_{01v}|^2 |x_{iu} - x_{il}| |x_{ju} - x_{jl}| \Delta x^2} \times \int_0^{t-t_k} \left\{ S_x^{\text{Jf}}(x_{il}, x_{jl}, x_{iu}, x_{ju}, \tau) + S_y(y_v, \tau) + S_z^{\text{Jf}}(z_{01}, z_{02}, z_{01}, z_{02}, \tau) \right\} d\tau$$

for $j = 1, \dots, N$ where $\Delta q_{fjk} = q_{fjk} - q_{fjk-1}$. An expression can also be written down for the average pressure at the wellbore given a rate history for each fracture segment in the form:

(21)

$$p(x_v, y_v, t) = p_I + \sum_{i=1}^N \sum_{k=1}^M \frac{\Delta q_{fik} U(t - t_k) d}{\pi^3 bc_r \phi |z_{02v} - z_{01v}|^2 |x_{iu} - x_{il}| \Delta x} \times \int_0^{t-t_k} \left\{ S_x^{\text{Jf}}(x_v, x_{il}, x_{iu}, \tau) + S_y(y_v, \tau) + S_z^{\text{Jf}}(z_{01}, z_{02}, z_{01}, z_{02}, \tau) \right\} d\tau$$

An expression can then be written down using the formation flow equations for the pressure drop between the wellbore and fracture segment j at time t_k :

(22)

$$\begin{aligned}
p(x_v, y_v, t_k) - p_{ff}(t_k) &= \sum_{i=1}^N \sum_{k=1}^M \frac{\Delta q_{fik} U(t-t_k) d}{\pi^3 b c_f \phi |z_{02v} - z_{01v}|^2 \Delta x} \times \\
&\times \int_0^{t-t_j} \left\{ S_x^{\downarrow} (x_v, x_{il}, x_{iu}, \tau) + S_y (y_v, \tau) + S_z^{\downarrow\downarrow} (z_{01}, z_{02}, z_{01}, z_{02}, \tau) \right\} d\tau - \\
&- \sum_{i=1}^N \sum_{k=1}^M \frac{2\Delta q_{fik} U(t-t_k) ad}{\pi^4 b c_f \phi |z_{02v} - z_{01v}|^2 \Delta x^2} \times \\
&\times \int_0^{t-t_j} \left\{ S_x^{\downarrow\downarrow} (x_{il}, x_{jl}, x_{iu}, x_{ju}, \tau) + S_y (y_v, \tau) + S_z^{\downarrow\downarrow} (z_{01}, z_{02}, z_{01}, z_{02}, \tau) \right\} d\tau
\end{aligned}$$

In the next section we will use a Fracture Flow Model to derive a corresponding equation for the pressure drop between the wellbore and fracture segment j . We will see later how these equations can be equated in order to solve for the rate history of each fracture segment which will enable us to derive our fractured well pressure as a function of time.

Fracture Flow Model

Non-Darcy flow within the fracture is described by Forchheimer's equation:

$$(23) \quad \frac{\partial p_f}{\partial x} = \frac{\mu b_f}{\sigma_f} V + \rho \beta V^2$$

where p_f is the pressure as a function of position and time within the fracture, μ and ρ are the fluid viscosity and density, σ_f and b_f the fracture conductivity and thickness, V the fluid velocity and β is the so-called "Beta factor" which quantifies the amount of non-Darcy flow. Setting $\beta = 0$ one recovers the familiar law of Darcy.

We assume that all fluid flows along the fracture in a direction perpendicular to the well at the fracture centre implying that the pressure within the fracture is a function of x and t only, $p_f(x, t)$. Strictly speaking this means that we must model a fracture that fully penetrates our reservoir as otherwise the pressure within the fracture would not be independent of y . We find however that assuming $p_f = p_f(x, t)$ is a good assumption as long as the fracture penetrates a reasonably large fraction of the formation.

We also note that the fluid velocity, $V = q_c(x, t) / b_f h$, where $q_c(x, t)$ is the cumulative fluid flow rate at time t that passes the point x within the fracture on its way to the well. Substituting for V in equation (23) we obtain:

$$(24) \quad \frac{\partial p_f}{\partial x} = \frac{\mu q_c(x, t)}{\sigma_f (z_{02v} - z_{01v})} + \frac{\rho \beta q_c^2(x, t)}{b_f^2 (z_{02v} - z_{01v})^2}$$

We assume that no fluid flows into the fracture at the fracture tip and that all the fluid is eventually produced up the well resulting in the following conditions:

$$\frac{\partial p_c(x_v + x_f, t)}{\partial x} = 0$$

$$\frac{\partial p_c(x_v, t)}{\partial x} = \frac{q_f}{2}$$

As in Guppy et al¹⁷. we assume that $q_c(x, t)$ varies linearly within a fracture segment and therefore we define it with the functional form:

$$(25) \quad q_c(x, t) = q_{ci}(t) + \left(\frac{q_{ci+1}(t) - q_{ci}(t)}{\Delta x} \right) \left(x - x_i + \frac{\Delta x}{2} \right)$$

where Δx is the size of each segment, $q_{ci+1}(t)$ is the value of the cumulative flux at the interface between segments i and $i+1$ and $q_{ci}(t)$ is the value of the cumulative flux at the interface between segments $i-1$ and i .

The pressure drop at the centre of segment i (relative to the well pressure) can then be found by integrating equation (24) so that:

$$(26) \quad \begin{aligned} &p_f(x_v, y_v, t) - p_f(x_i, t) \\ &= \frac{\mu}{\sigma_f (z_{02v} - z_{01v})} \int_{x_v}^{x_i} q_c dx' + \frac{\rho \beta}{b_f^2 (z_{02v} - z_{01v})^2} \int_{x_v}^{x_i} q_c^2 dx' \end{aligned}$$

We then sum the resulting pressure drops from each fracture segment so that equation (26) transforms into:

$$(27) \quad \begin{aligned} &p_f(x_v, y_v, t) - p_f(x_i, t) = \frac{\mu}{\sigma_f (z_{02v} - z_{01v})} \times \\ &\times \left(\sum_{i=1}^{j-1} \int_{x_i - \Delta x/2}^{x_i + \Delta x/2} q_{ci} dx + \int_{x_j - \Delta x/2}^{x_j} q_{cj} dx \right) + \\ &+ \frac{\rho \beta}{b_f^2 (z_{02v} - z_{01v})^2} \times \\ &\times \left(\sum_{i=1}^{j-1} \int_{x_i - \Delta x/2}^{x_i + \Delta x/2} q_{ci}^2 dx + \int_{x_j - \Delta x/2}^{x_j} q_{cj}^2 dx \right) \end{aligned}$$

where q_{cj} is the cumulative fluid flow rate across the interface between fracture segment j and $j-1$. Using equation (25) to substitute for each q_{cj} at a specific timestep t_k and evaluating the integrals yields:

$$(28) \quad p_f(x_v, y_v, t_k) - p_f(x_i, t_k) = \frac{\mu}{\sigma_f(z_{02v} - z_{01v})} T_D + \frac{\rho\beta}{b_f^2(z_{02v} - z_{01v})^2} T_{ND}$$

where T_D and T_{ND} are terms representing the Darcy and non-Darcy terms respectively and are defined:

$$(29) \quad T_D = \sum_{i=1}^{j-1} \left(q_{ci}(t_k) \frac{\Delta x}{2} + q_{ci+1}(t_k) \frac{\Delta x}{2} \right) + q_{cj}(t_k) \frac{3\Delta x}{8} + q_{cj+1}(t_k) \frac{\Delta x}{8} + q_{cj}^2(t_k) \frac{7\Delta x}{24} + q_{cj+1}^2(t_k) \frac{\Delta x}{24} + q_{cj+1}(t_k) q_{cj}(t_k) \frac{\Delta x}{6}$$

$$(30) \quad T_{ND} = \sum_{i=1}^{j-1} \left(q_{ci}^2(t_k) \frac{\Delta x}{3} + q_{ci}(t_k) q_{ci+1}(t_k) \frac{\Delta x}{3} + q_{ci+1}^2(t_k) \frac{\Delta x}{3} \right)$$

Solution Formulation

We proceed by equating the pressure drop in equations (22) and (28) which were derived using the Formation Flow Model and the Fracture Flow Model respectively. In order to do this we note that the cumulative flux in the fracture is related to the flux into each fracture segment by the simple relationship:

$$(31) \quad q_{fjk} = q_{cj+1}(t_k) - q_{cj}(t_k)$$

Substituting for q_{fjk} in equation (22) and then equating equations (22) and (28) gives us our final expression:

$$(32) \quad \frac{\mu}{\sigma_f(z_{02v} - z_{01v})} T_D + \frac{\rho\beta}{b_f^2(z_{02v} - z_{01v})^2} T_{ND} - \sum_{i=1}^N \sum_{k=1}^M \frac{2[q_{ci+1}(t_k) - q_{ci}(t_k) - q_{ci+1}(t_{k-1}) + q_{ci}(t_{k-1})] U(t-t_k) d}{\pi^3 b_{ci} \phi |z_{02v} - z_{01v}|^2 \Delta x} \times \int_0^{t-t_j} \left\{ S_x^j(x_v, x_{il}, x_{iu}, \tau) + S_y(y_v, \tau) + S_z^j(z_{01}, z_{02}, z_{01}, z_{02}, \tau) \right\} d\tau + \sum_{i=1}^N \sum_{k=1}^M \frac{2[q_{ci+1}(t_k) - q_{ci}(t_k) - q_{ci+1}(t_{k-1}) + q_{ci}(t_{k-1})] U(t-t_k) db}{\pi^4 c_i \phi |z_{02v} - z_{01v}|^2 \Delta x^2} \times \int_0^{t-t_j} \left\{ S_x^{jj}(x_{il}, x_{jl}, x_{iu}, x_{ju}, \tau) + S_y(y_v, \tau) + S_z^j(z_{01}, z_{02}, z_{01}, z_{02}, \tau) \right\} d\tau = 0$$

for $j = 2, \dots, N$ i.e. $N-1$ equations. Each equation contains $N-1$ unknowns at each timestep, t_k , which are the cumulative fluxes $q_{c2}(t_k), q_{c3}(t_k), \dots, q_{cN}(t_k)$. We have successfully used Newton's method to solve this system of non-linear equations to obtain the set of cumulative fluxes at each timestep. Once they are known then the average well pressure can be obtained using the equation:

$$(33) \quad p(x, y, t) = p_l + \sum_{i=1}^N \sum_{k=1}^M \frac{\Delta q_{fik} U(t-t_k) d}{\pi^3 b_{ci} \phi |z_{02v} - z_{01v}|^2 \Delta x} \times \int_0^{t-t_j} \left\{ S_x^j(x, x_{li}, x_{ui}, \tau) + S_y(y, \tau) + S_z^j(z_{01}, z_{02}, z_{01}, z_{02}, \tau) \right\} d\tau$$

and choosing suitable values of x and y using the known well radius.

Development of the Solutions in Laplace Space

Analytical solutions in Laplace space have been well documented in the literature and open up the possibility to model wellbore storage, naturally fractured reservoirs, non-Darcy flow in wells and wells operating under constant pressure production. However, there are severe computational problems associated with evaluating analytic Laplace space solutions of this nature, as described for example in Ozkan and Raghavan¹⁸.

Appendix B gives an example of the computational issues associated with such solutions by considering the analytic solution in Laplace space of the single rate vertical well problem. It is clearly illustrated that calculating the series solution is completely impractical and that another approach is necessary.

Our solution deals with this problem in a simple but elegant way and can cope with all time ranges of interest. Let us return to the problem of the single rate vertical well problem in equation (11). We can perform the Laplace transform of this equation numerically so that:

(34)

$$\bar{p}_v(x, y, s) = \frac{p_l}{s} + \frac{qd}{2\pi^2 abc_t \phi |z_{02v} - z_{01v}|^2} \int_0^\infty e^{-st} \int_0^t f(\tau) d\tau dt$$

$$\text{where } f(\tau) = \left\{ S_x(x, \tau) + S_y(y, \tau) + S_z^{\text{II}}(z_{01}, z_{02}, z_{01}, z_{02}, \tau) \right\}$$

Using standard properties of the Laplace transform, equation (34) can be reduced to the form:

(35)

$$\bar{p}_v(x, y, s) = \frac{p_l}{s} + \frac{qd}{2s\pi^2 abc_t \phi |z_{02v} - z_{01v}|^2} \int_0^\infty e^{-st} f(t) dt$$

meaning we now only have to perform one integral over time. Equation (35) can then be rewritten in the form:

(36)

$$\bar{p}_v(x, y, s) - \frac{p_l}{s} = \frac{qd}{2s\pi^2 abc_t \phi |z_{02v} - z_{01v}|^2} \times \left(\int_0^T e^{-st} f(t) dt + \int_T^\infty e^{-st} f(t) dt \right)$$

We now use the fact that over the range $0 < t < T$ (for a carefully chosen value of T) the term e^{-st} is approximately constant and can therefore be brought outside the integral to yield:

(37)

$$\bar{p}_v(x, y, s) - \frac{p_l}{s} \approx \frac{qd}{2s\pi^2 abc_t \phi |z_{02v} - z_{01v}|^2} \times \left(e^{-sT/2} \int_0^T f(t) dt + \int_T^\infty e^{-st} f(t) dt \right)$$

We find setting $T = 1/(ns)$ gives good results where n is the value of n used in the Stehfest¹⁵ inversion algorithm given by:

$$(38) \quad p_v(x, y, t) = \frac{\ln 2}{t} \sum_{i=1}^n V_i p \left(x, y, \frac{\ln 2}{t} i \right)$$

Finally, we re-write the second integral in equation (37) to obtain:

(39)

$$\bar{p}_v(x, y, s) - \frac{p_l}{s} \approx \frac{qd}{2s\pi^2 abc_t \phi |z_{02v} - z_{01v}|^2} \times \left(e^{-sT/2} \int_0^T f(t) dt + \frac{1}{s} \int_0^\infty e^{-(t+sT)} f \left(\frac{t}{s} + T \right) dt \right)$$

Equation (34) gives huge computational gains when re-written in the form of equation (39). The fact that the first integral is not dependent on s means that previous evaluations of the integral for other values of s can be re-used. This can be exploited to maximum effect by performing the sum in equation (39) from $i = N, \dots, 1$.

The second integral in equation (36) is in a form suitable for use with the Gauss-Laguerre integration algorithm¹⁹ since the integrand decays exponentially over the range of t of interest. Given a number of points to use in the integration, the Gauss-Laguerre algorithm requires the weights used in the calculation to be computed just once. Any subsequent integrals to be evaluated can then use these pre-calculated weights. We have found that as few as 15 points are required to compute this integral accurately using the Gauss-Laguerre algorithm making it an extremely cheap calculation.

Our method therefore offers very fast calculation of well pressures in Laplace space over all time ranges of interest. There have been other attempts in the literature to obtain well pressures in Laplace space by numerically transforming the real time well pressures such as in Thompson et al¹⁴. However, this method relies on pre-calculated tables of the real time well pressure, whereas our method requires no such a-priori knowledge without the speed of the calculation being compromised.

Problems involving wellbore storage, constant pressure production, non-Darcy flow and that of naturally fractured mediums can now be easily computed as outlined in Ozkan & Raghavan¹⁸ or Sabet¹⁵. For example, van Everdingen and Hurst²⁰ showed that the pressure response of a well with wellbore storage coefficient C can be written in the form:

$$(40) \quad \bar{p}_v(x, y, s) = q \frac{\bar{p}_{ur}}{1 + s^2 C \bar{p}_{ur}}$$

where \bar{p}_{ur} is the Laplace transform of the unit rate pressure response of a well without wellbore storage and is defined:

(41)

$$\bar{p}_{ur}(x, y, s) = \frac{d}{2s\pi^2 abc_t \phi |z_{02v} - z_{01v}|^2} \int_0^\infty e^{-st} f(t) dt$$

As already outlined, equation (39) can be used to calculate the pressure response in Laplace space for a well producing at constant rate $q\sqrt{vt}$. If we allow a series of Heaviside step function based rates to be used for the rate history of the well, as in equation (12), then our Laplace space solution will be written:

$$(42) \quad \bar{p}_v(x, y, s) = \frac{p_I}{s} + \frac{d}{2s\pi^2 abc_f \phi |z_{02v} - z_{01v}|^2} \times \left\{ \sum_{j=0}^N \Delta q_j e^{-st_j} \right\} \int_0^{\infty} e^{-st} f(t) dt$$

There are problems associated with using the Stehfest²¹ inversion algorithm on equation (42) due to the discontinuous nature of the rate history. The solution, as outlined in a very elegant approach by Chen & Raghavan²², is to superpose N different Laplace space functions, each function having its own Laplace variable s_j . The Stehfest algorithm can then be used to invert each Laplace function individually to obtain a set of N real time pressure responses which can simply be added to obtain the total real time pressure response of the well. Chen & Raghavan's method can be used to write the Laplace space pressure response due to the entire rate history of the well as:

$$(43) \quad \bar{p}(x, y, s) = \frac{p_I}{s} + \sum_{j=1}^N \frac{t}{t - t_{j-1}} \Delta q_j \bar{p}_{ur}(x, y, s_j)$$

where s_j is the j th Laplace variable, based on the elapsed time $t - t_{j-1}$.

Validation and Application

The algorithms were validated against special cases of the solution of the diffusivity equation for a single well. All well test interpretation software packages have these solutions; we used Weltest 200*. Subsequently, for multiple well situations with long pressure production history, numerical simulation results were used. We used the ECLIPSE* reservoir simulator to build our numerical models.

A comprehensive sets of tests were carried out. We present a few examples to demonstrate the speed and accuracy of our algorithms. Figures 3 and 4 present pressure and log-log pressure derivative plots respectively corresponding to a well test. It can be seen that our generalized solution reduces to the specific channel sand solution.

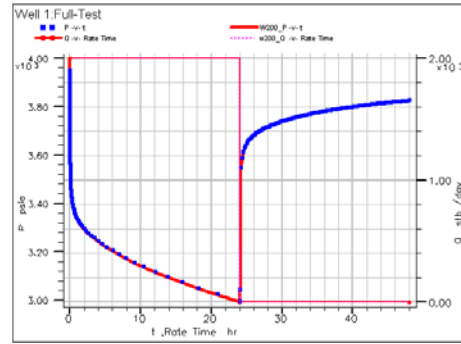


Figure 3: Pressure response in channel

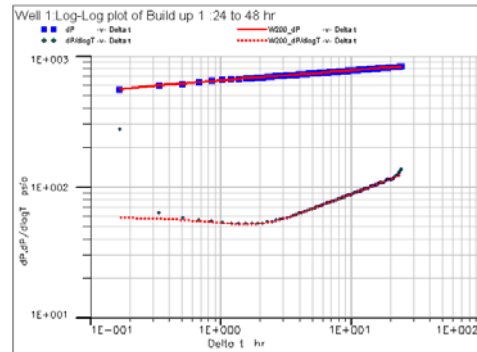


Figure 4: Log-log plot for pressure response in channel

In order to provide a solid test of our semi-analytic model for a finite conductivity fracture we used a fracture with a very low dimensionless conductivity, $\sigma_{FD} = k_f b_f / kx_f = 0.004$.

This ensures that the pressure derivative response is significantly affected by the flow in the fracture itself. We have found agreement with the conclusions of Guppy¹⁷ in that for low dimensionless fracture conductivities we need about 30 fracture segments to yield accurate results. In Figure 5 we show a log-log plot of our results compared to that of Weltest 200*.

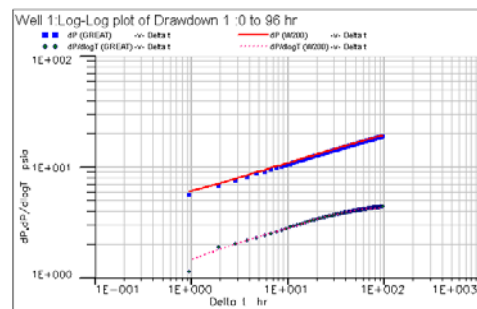


Figure 5: Log-log plot for pressure response in hydraulically fractured well

Figure 6 shows the effect of non-Darcy flow in a fracture. Please note how the pressure drop increases with an increase in mesh size. The beta factor, which quantifies the degree of non-Darcy flow, is related to the mesh size by the formula of Cooke²³.

* Mark of Schlumberger

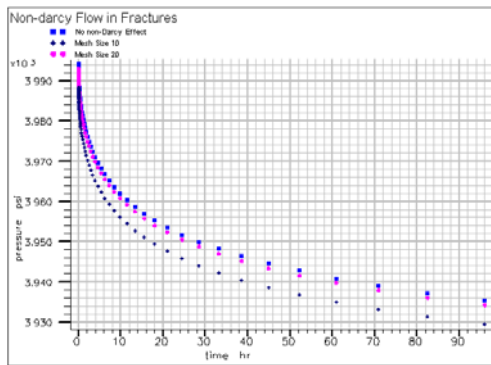


Figure 6: Effect of non-Darcy flow on pressure response for a fractured well

Figure 7 shows a numerical simulation model of a rectangular reservoir with 25 wells. 12 of the wells are fractured and an observation well is placed at the centre of the reservoir.

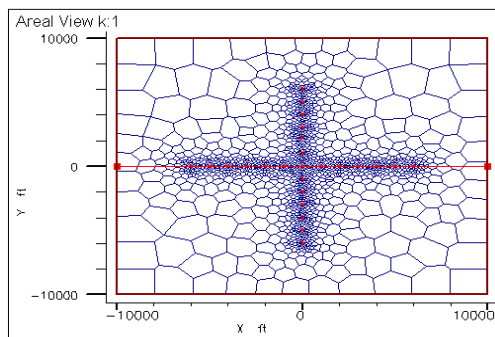


Figure 7: Unstructured grid for the simulation model

As can be seen in the bottom hole pressure plot of the observation well (Figure 8), an excellent match is obtained between our algorithm and the numerical model. The execution time for our model was less than 20 seconds compared to more than 1.7 hours (6277 secs) for the numerical model – a gain of a factor of more than 300. Please note that the fractures were explicitly modeled in the numerical model.

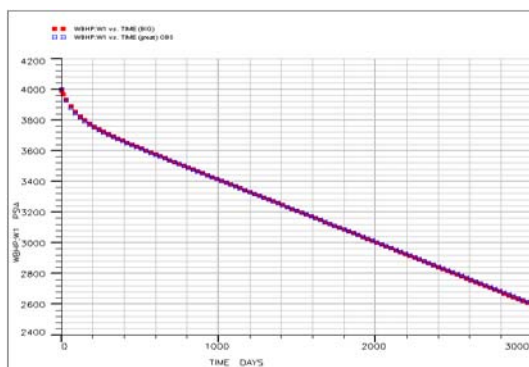


Figure 8: Pressure response at the observation well

In order to perform automatic history match history we incorporated a gradient-based optimization routine into our software. In order to test our approach we obtained synthetic well bottom hole pressure and rate response from a numerical

simulation model containing 3 wells. Thus we had a-priori knowledge of the values of the history matching parameters.

The parameters in this case were k_x , k_y , k_z and well skins.

We perturbed the values of these parameters in our model, used the synthetic simulation result as observed data and ran the model through a regression loop. A very good match was obtained for each of the wells. Figure 9 shows the match for one of the wells. The matched parameters were within 1 percent of the model parameters used to generate the data.

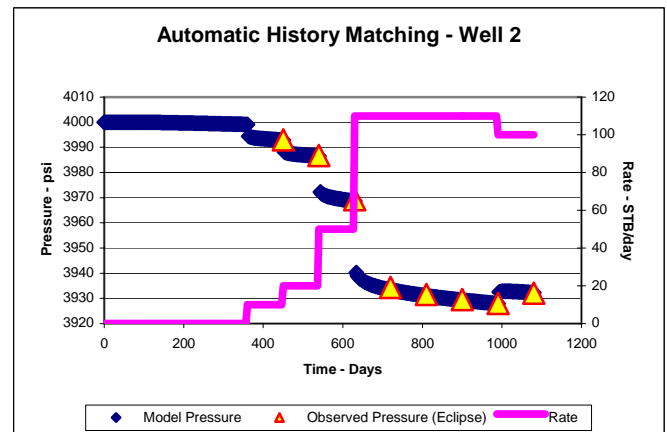


Figure 9: Bottom hole pressure match for Well2.

Our method has been implemented in the form of a software library with a well-defined API. We see a number of applications that could use this library. Firstly, it can be used as a proxy simulator. This includes integration with a pipeline network simulator for asset management particularly in the case of gas reservoirs. Moreover, simplicity and speed makes the software useful for real-time application. Real-time well diagnostics using permanent downhole gauges is an ideal application. On a different note, a production engineer could use it to quickly evaluate hydrocarbon reservoirs, perhaps as a precursor to detailed full-field numerical simulation. Finally, one may use the library in a well test interpretation package as a generalized well test model allowing, among others, interference tests and wireline formations tests.

Conclusions

In this paper we have outlined the mathematics of a generalized single layer analytical model that models multi-well (horizontal and vertical) single layer reservoir problems. The following results were outlined:

- Derivation of a solution to the diffusivity equation for problems with a large variety of boundary and initial conditions. We showed an example of a solution where Neumann (flux) boundary conditions were specified on each side of our single layer reservoir. However, the integral transform technique of Thambayagam⁷ can be used to solve problems where any permutation of the Neumann (flux), Dirichlet (pressure) and Robin (flux+pressure) conditions are specified over the 6 boundaries.

- A mathematical model for both infinite conductivity (uniform flux) and finite conductivity fractures with non-Darcy flow in the context of our multi-well closed box reservoir.
- A methodology for efficiently computing Laplace solutions. This enabled us to model physical effects such as constant pressure production and wellbore storage.
- The algorithm achieves excellent accuracy with massive speed gains over numerical finite difference based simulators.
- Combined with a gradient-based optimizer algorithm it also proves a powerful tool for performing very fast history matching studies.

We see a number of possible use of our algorithm. It could be used for production evaluation, as a proxy to numerical simulator and as a generalized well test model.

Nomenclature

- a = reservoir length
 b = reservoir width
 b_f = fracture thickness
 C = wellbore storage coefficient
 c_o = fluid compressibility
 c_R = rock compressibility
 c_t = total formation (fluid + rock) compressibility
 d = reservoir height
 k_x = permeability in the x -direction
 k_y = permeability in the y -direction
 k_z = permeability in the z -direction
 k_f = fracture permeability
 p_I = initial well/reservoir pressure
 $p_f(x, t)$ = fracture pressure as a function of position and time
 $p_v(x, y, t)$ = average pressure of a vertical well at point (x, y) at time t
 $\bar{p}_v(x, y, s)$ = Laplace transform of the average pressure of a vertical well at point (x, y)
 $q_c(x, t)$ = cumulative fluid flow rate passing point x at time t
 $q_{c_j}(t)$ = cumulative fluid flow rate across the interface between fracture segment j and $j-1$
 q_{fjk} = flow rate into fracture segment j at time interval k
 Δq_j = difference between the flow rate at time j and $j-1$
 s = Laplace variable corresponding to elapsed time t
 s_j = Laplace variable corresponding to elapsed time $t-t_j$
 x_{0p} = x coordinate of a point source

- x_f = fracture half-length
 x_{01h} = lower x coordinate of a horizontal well
 x_{02h} = upper x coordinate of a horizontal well
 x_{0v} = x coordinate of a vertical well
 y_{0v} = y coordinate of a vertical well
 y_{0h} = y coordinate of a horizontal well
 y_{0p} = y coordinate of a point source
 z_{0h} = z coordinate of a horizontal well
 z_{01v} = lower z coordinate of a vertical well
 z_{02v} = upper z coordinate of a vertical well
 z_{0p} = z coordinate of a point source
 β = non-Darcy Beta factor
 μ = fluid viscosity
 ϕ = porosity
 ϕ_f = fracture porosity
 $\varphi(x, y, z)$ = initial reservoir pressure as a function of position
 η_x = diffusivity constant in the x direction
 η_y = diffusivity constant in the y direction
 η_z = diffusivity constant in the z direction
 σ_f = fracture conductivity
 σ_{fD} = dimensionless fracture conductivity

Acknowledgement

The authors thank Schlumberger for permission to publish this paper. The authors also acknowledge the contribution of Philip Gilchrist in implementation of parts of the algorithm.

References

1. Sneddon, I.N.: “*The Use of Integral Transforms*”, McGraw-Hill Book Company, New York (1972).
2. Churchill, R.V.: “*Extensions of Operational Mathematics*”, Proc. Conf. Diff. Eqns., University of Maryland Bookstore (1955).
3. Churchill, R.V.: “*Operational Mathematics*”, second edition, McGraw-Hill Publishing Company, New York (1958).
4. Tranter, C.J.: “*Integral Transforms in Mathematical Physics*”, John Wiley & Sons, Inc, New York, (1951).
5. Titchmarsh, E.C.: “*Fourier Integrals*”, Clarendon Press, Oxford, (1962).
6. Korner, T.W.: “*Fourier Analysis*”, Cambridge University Press, Cambridge, (1988).
7. Thambayagam, R.K.M.: “*Diffusion: A Compendium of Analytical Solutions*”, TBP.
8. Al-Hussainy, R., Ramey, H.J. Jr., Crawford, P.B.: “*The Flow of Real Gases Through Porous Media*”, Trans. SPE of AIME, **18**, (1966) 624.

9. Agarwal, R.G.: “*Real Gas Pseudo-Time – A New Function For Pressure Buildup Analysis of MHF Gas Wells*”, paper SPE 8279 presented at SPE Annual Technical Conference and Exhibition, Las Vegas, Nevada, 23-26 Sep 1979.
10. Aziz, K., Settari, A.: “*Petroleum Reservoir Simulation*”, Published by Khalid Aziz and Antonin Settari, (1979).
11. Babu, D.K., Odeh, A.S.: “*Productivity of a Horizontal Well*”, SPE (Nov 1989) 417.
12. Babu D.K., Odeh, A.S.: “*Appendices of SPE 18298*”, SPE 18334, (1988).
13. Mutalik, P.N., Godbole, S.P., Joshi, S.D.: “*Effect of Drainage Area Shapes on the Productivity of Horizontal Wells*”, paper SPE 18301 presented at SPE Annual Technical Conference and Exhibition, Houston, Texas, 2-5 Oct. 1988.
14. Thompson, L.G., Manrique, J.L.: “*Efficient Algorithms for Computing the Bounded Horizontal Well Pressure Response*”, paper SPE 21827 presented at Low Permeability Reservoirs Symposium, Denver, Colorado 15-17 April, 1991.
15. Sabet, M.A.: “*Well Test Analysis*”, Gulf Publishing Company, (1991).
16. Gringarten, A.C., Ramey, J.R., Henry J.: “*Unsteady State Pressure Distributions Created by a Well With a Single Infinite-Conductivity Vertical Fracture*”, SPEJ (Aug. 1974) 347.
17. Guppy, K.H., Cinco-Ley, Ramey Jr., H.J., Samaniego-V., F.: “*Non-Darcy Flow in Wells With Finite-Conductivity Vertical Fractures*”, SPEJ (Oct. 1982) 681.
18. Ozkan, E., Raghavan, R.: “*New Solutions for Well-Test Analysis Problems: Part 2 – Computational Considerations and Applications*”, SPEFE (Sep. 1991) 369.
19. Press, W.H., Vetterling, W.T., Teukolsky, S.A., Flannery, B.P.: “*Numerical Recipes in C*”, Second Edition, Cambridge University Press, Cambridge, (1988).
20. Van Everdingen, A.F. and Hurst, W.: “*The Application of the Laplace Transformation to Flow Problems in Reservoirs*”, Trans. AIME, 186, (1949) 305.
21. Stehfest, H., “*Numerical Inversion of Laplace Transforms*”, Communications of the ACM, **13**, No.1, (1970) 47.
22. Chen, C., Raghavan, R.: “*An Approach to Handle Discontinuities by the Stehfest Algorithm*”, SPEJ (Dec. 1996) 363.
23. Cooke, C.E. Jr.: “*Conductivity of Fracture Proppants in Multiple Layers*”, JPT (Sep. 1973) 1101
24. Abramowitz, M., & Stegun, I.A.: “*Handbook of Mathematical Functions*”, Dover Publications, (1972).
25. Spanier, J. & Oldham, K.B.: “*An Atlas Of Functions*”, Hemisphere Publishing Corporation, (1987).

Appendix A Solution of the Diffusivity Equation

In this appendix we outline the derivation of the solution of the diffusivity equation for a single, partially penetrating, vertical well. We start by considering the case of a point source at (x_{0p}, y_{0p}, z_{0p}) which produces a quantity of fluid Q at $t = t_0$. The resulting pressure response in the reservoir will satisfy the diffusivity equation:

$$(42) \quad \frac{\partial p}{\partial t} = \eta_x \frac{\partial^2 p}{\partial^2 x} + \eta_y \frac{\partial^2 p}{\partial^2 y} + \eta_z \frac{\partial^2 p}{\partial^2 z} + \frac{Q}{\phi c_t} \delta(x - x_{0p}) \delta(y - y_{0p}) \delta(z - z_{0p})$$

where $\eta_x = k_x / \phi c_t \mu$, $\eta_y = k_y / \phi c_t \mu$, $\eta_z = k_z / \phi c_t \mu$ and are the diffusivity constants in the x , y , z directions respectively.

Our single layer (box) reservoir has length a , width b and height d with porosity ϕ and permeabilities k_x , k_y , k_z in the x , y and z directions respectively. In this particular example we impose flux or Neumann-type boundary conditions on each of the six boundaries of the reservoir so that:

$$(43) \quad \frac{\partial p(0, y, z, t)}{\partial x} = - \left(\frac{\mu}{k_x} \right) \psi_{0yz}(y, z, t)$$

$$(44) \quad \frac{\partial p(a, y, z, t)}{\partial x} = - \left(\frac{\mu}{k_x} \right) \psi_{ayz}(y, z, t)$$

$$(45) \quad \frac{\partial p(x, 0, z, t)}{\partial y} = - \left(\frac{\mu}{k_y} \right) \psi_{x0z}(x, z, t)$$

$$(46) \quad \frac{\partial p(x, b, z, t)}{\partial y} = - \left(\frac{\mu}{k_y} \right) \psi_{xbz}(x, z, t)$$

$$(47) \quad \frac{\partial p(x, y, 0, t)}{\partial z} = - \left(\frac{\mu}{k_z} \right) \psi_{xy0}(x, y, t)$$

$$(48) \quad \frac{\partial p(x, y, d, t)}{\partial z} = - \left(\frac{\mu}{k_z} \right) \psi_{xyd}(x, y, t)$$

where for instance $\psi_{0yz}(y, z, t)$ is the flux as a function of position across the (y, z) plane at $x = 0$.

We note that the Laplace transform of a function, $\bar{f}(s)$ is defined as:

$$(49) \quad \bar{f}(s) = \int_0^{\infty} f(t) e^{-st} dt$$

We apply the Laplace transform to equation (42) which gives us an expression in terms of $\bar{p}(x, y, z, s)$ in the form:

$$(50) \quad \eta_x \frac{\partial^2 \bar{p}}{\partial^2 x} + \eta_y \frac{\partial^2 \bar{p}}{\partial^2 y} + \eta_z \frac{\partial^2 \bar{p}}{\partial^2 z} - s\bar{p} = - \frac{Q}{\phi c_t} \delta(x - x_{0p}) \delta(y - y_{0p}) \delta(z - z_{0p}) e^{-st_0} - \phi(x, y, z)$$

where $\phi(x, y, z)$ is the initial pressure of the reservoir. We also note that the finite cosine Fourier transform of a function, $\bar{f}(s)$, is defined as:

$$(51) \quad \bar{f}(n) = \int_0^a f(x) \cos\left(\frac{(2n-1)\pi x}{2a}\right) dx$$

with its inversion formula by:

$$(52) \quad f(x) = \frac{1}{a} \bar{f}(0) + \frac{2}{a} \sum_{n=1}^{\infty} \bar{f}(n) \cos\left(\frac{n\pi x}{a}\right)$$

We now apply successive Fourier transforms with respect to the x , y and z variables respectively to obtain an expression for $\bar{\bar{\bar{p}}}_v = \bar{\bar{\bar{p}}}_v(n, m, l, s)$ in the form:

$$(53) \quad \bar{\bar{\bar{p}}}_v = \frac{Q \cos\left(\frac{n\pi x_{0p}}{a}\right) \cos\left(\frac{m\pi y_{0p}}{b}\right) \cos\left(\frac{l\pi z_{0p}}{d}\right) e^{-st_0}}{\phi c_t \left\{ \eta_x \left(\frac{n\pi}{a}\right)^2 + \eta_y \left(\frac{m\pi}{b}\right)^2 + \eta_z \left(\frac{l\pi}{d}\right)^2 + s \right\}} - \frac{\left\{ (-1)^{n+1} \bar{\bar{\bar{\psi}}}_{ayz}(m, l, s) + \bar{\bar{\bar{\psi}}}_{0yz}(m, l, s) \right\}}{\phi c_t \left\{ \eta_x \left(\frac{n\pi}{a}\right)^2 + \eta_y \left(\frac{m\pi}{b}\right)^2 + \eta_z \left(\frac{l\pi}{d}\right)^2 + s \right\}} - \frac{\left\{ (-1)^{m+1} \bar{\bar{\bar{\psi}}}_{xbz}(n, l, s) + \bar{\bar{\bar{\psi}}}_{x0z}(n, l, s) \right\}}{\phi c_t \left\{ \eta_x \left(\frac{n\pi}{a}\right)^2 + \eta_y \left(\frac{m\pi}{b}\right)^2 + \eta_z \left(\frac{l\pi}{d}\right)^2 + s \right\}} - \frac{\left\{ (-1)^{l+1} \bar{\bar{\bar{\psi}}}_{xyd}(n, m, s) + \bar{\bar{\bar{\psi}}}_{xy0}(n, m, s) \right\}}{\phi c_t \left\{ \eta_x \left(\frac{n\pi}{a}\right)^2 + \eta_y \left(\frac{m\pi}{b}\right)^2 + \eta_z \left(\frac{l\pi}{d}\right)^2 + s \right\}} + \frac{\int_0^a \int_0^b \int_0^d \varphi(u, v, w) \cos\left(\frac{n\pi u}{a}\right) \cos\left(\frac{m\pi v}{b}\right) \cos\left(\frac{l\pi w}{d}\right) du dv dw}{\left\{ \eta_x \left(\frac{n\pi}{a}\right)^2 + \eta_y \left(\frac{m\pi}{b}\right)^2 + \eta_z \left(\frac{l\pi}{d}\right)^2 + s \right\}}$$

where the functions $\bar{\bar{\bar{\psi}}}_{ayz}(m, l, s)$, $\bar{\bar{\bar{\psi}}}_{0yz}(m, l, s)$, etc. involve Fourier transforms of the various boundary flux functions and are defined in appendix C. We then apply successive inverse Fourier transforms and an inverse Laplace transform to obtain a solution for the pressure at any point in the reservoir, $p(x, y, z, t)$ in the form:

$$(54) \quad p(x, y, z, t) = \frac{U(t-t_0)Q}{8abd c_t \phi} \int_0^{t-t_0} \left\{ S_x(x, x_{0p}, \tau) S_y(y, y_{0p}, \tau) S_z(z, z_{0p}, \tau) \right\} d\tau + \frac{4}{\phi c_t a b d} \int_0^t \left\{ B_x(x, y, z, \tau) + B_y(x, y, z, \tau) + B_z(x, y, z, \tau) \right\} d\tau + \frac{1}{8abd} \int_0^a \int_0^b \int_0^d \varphi(u, v, w) \left\{ I_x(u, x) I_y(v, y) I_z(w, z) \right\} du dv dw$$

where $\varphi(x, y, z) = p(x, y, z, 0)$ and describes the initial pressure of the reservoir. We refer to the first term as the source term which describes the pressure contribution from the point source. The second term we call the boundary term since it describes the pressure contribution due to the fluid flow across the boundaries. Finally, the third term is the initial term which dictates the pressure contribution due to the initial conditions of the reservoir. The source functions, $S_x(x, x_{0p}, \tau)$, $S_y(y, y_{0p}, \tau)$, $S_z(z, z_{0p}, \tau)$, boundary functions, $B_x(x, \tau)$, $B_y(y, \tau)$, $B_z(z, \tau)$ and initial functions, $I_x(u, x)$, $I_y(v, y)$, $I_z(w, z)$ are defined in Appendix C.

Part of the power of equation (54) is that each of the source, boundary and initial terms can be integrated multiple times depending on the problem involved. To describe a vertical well producing at rate $q(t)$ for $t > t_0$ we integrate the source terms over the appropriate time interval and integrate the term $S_z(z, z_{0p}, \tau)$ over z_{0p} from z_{01v} , the bottom end of the perforated vertical well, to z_{02v} , the top end. We then set $x_{0v} = x_{0p}$ and $y_{0v} = y_{0p}$, since the x and y positions of our line source will remain the same as that of the original point source. This yields:

$$\begin{aligned}
 (55) \quad p_v(x, y, t) = & \frac{U(t - t_0)}{4\pi abc_i \phi |z_{02v} - z_{01v}|} \int_0^{t-t_0} q(t - t_0 - \tau) \left\{ S_x(x, x_{0v}, \tau) S_y(y, y_{0v}, \tau) S_z(z_{01v}, z_{02v}, z, \tau) \right\} d\tau + \\
 & + \frac{4}{\phi c_i ab d} \int_0^t \left\{ B_x(x, y, z, \tau) + B_y(x, y, z, \tau) + B_z(x, y, z, \tau) \right\} d\tau + \\
 & + \frac{1}{8abd} \int_0^a \int_0^b \int_0^d \varphi(u, v, w) \left\{ I_x(u, x) I_y(v, y) I_z(w, z) \right\} dudvdw
 \end{aligned}$$

where $S_z(z_{01v}, z_{02v}, z, \tau)$ is also defined in Appendix C. Given that the pressure of a partially penetrating well will vary across the well itself we have found it most useful for practical applications to calculate the average well pressure. This is obtained by integrating equation (55) over the spatial interval of the well and then dividing by the well length yielding an expression for the average well pressure of our vertical well, which we will also denote $p_v(x, y, t)$:

$$\begin{aligned}
 (56) \quad p_v(x, y, t) = & \frac{U(t - t_0)d}{2\pi^2 abc_i \phi |z_{02v} - z_{01v}|^2} \int_0^{t-t_0} q(t - t_0 - \tau) \left\{ S_x(x, x_{0v}, \tau) S_y(y, y_{0v}, \tau) S_z(z_{01v}, z_{02v}, z_{01v}, z_{02v}, \tau) \right\} d\tau + \\
 & + \frac{4}{\phi c_i ab d |z_{02v} - z_{01v}|} \int_0^t \left\{ B_x(x, y, z_{01v}, z_{02v}, \tau) + B_y(x, y, z_{01v}, z_{02v}, \tau) + B_z(x, y, z_{01v}, z_{02v}, \tau) \right\} d\tau + \\
 & + \frac{1}{4ab\pi |z_{02v} - z_{01v}|} \int_0^a \int_0^b \int_0^d \varphi(u, v, w) \left\{ I_x(u, x) I_y(v, y) I_z(w, z_{01v}, z_{02v}) \right\} dudvdw
 \end{aligned}$$

We again refer the reader to Appendix C for definitions of the terms $S_z(z_{01v}, z_{02v}, z_{01v}, z_{02v}, \tau)$, $B_x(x, y, z_{01v}, z_{02v}, \tau)$, $B_y(x, y, z_{01v}, z_{02v}, \tau)$, $B_z(x, y, z_{01v}, z_{02v}, \tau)$ and $I_z(w, z_{01v}, z_{02v})$.

Appendix B Convergence Analysis of Analytic Laplace Space Solutions

In this appendix we investigate the convergence problems of analytic solutions in Laplace space. Our example is based on the single, partially penetrating, vertical well problem addressed by equation (13) in the main text. Taking the Laplace transform of this equation yields:

$$\begin{aligned}
 (57) \quad \bar{p}_v(x, y, s) = & \frac{2d \left\{ \sum_{j=0}^N q_j e^{-st_j} \right\}}{s\pi^2 b \phi c_i \eta_x |z_{02v} - z_{01v}|^2} \sum_{m=0}^{\infty} \sum_{l=0}^{\infty} \frac{\mathfrak{A}_m \mathfrak{A}_l \csc h \left\{ a \sqrt{\beta_x + \frac{s}{\eta_x}} \right\}}{l^2 \sqrt{\beta_x + \frac{s}{\eta_x}}} \left\{ \sin \left(\frac{l\pi z_{02v}}{d} \right) - \sin \left(\frac{l\pi z_{01v}}{d} \right) \right\}^2 \cos \left(\frac{m\pi y}{b} \right) \cos \left(\frac{m\pi y_{0v}}{b} \right) \times \\
 & \times \left[\cosh \left\{ (a - |x - x_{0v}|) \sqrt{\beta_x + \frac{s}{\eta_x}} \right\} + \cosh \left\{ (a - x - x_{0v}) \sqrt{\beta_x + \frac{s}{\eta_x}} \right\} \right]
 \end{aligned}$$

where:

$$(58) \quad \beta_x = \frac{\eta_y}{\eta_x} \left(\frac{m\pi}{b} \right)^2 + \frac{\eta_z}{\eta_x} \left(\frac{l\pi}{d} \right)^2$$

We set $m = 0$ and $\eta_x = \eta_y$ in equation (57) in order to investigate the convergence of the sum in l . The exponential behaviour of the sum in l is then:

$$(59) \quad \cosh \left\{ -|x - x_0| \sqrt{\beta_x + \frac{s}{\eta_x}} \right\} = \cosh \left\{ -l\pi \frac{|x - x_0|}{b} \right\}$$

which will control the convergence of the series in l . For the sake of illustration we choose some parameter values by setting the layer width, $b = 10^4 m$, and well radius, $x - x_0 = 0.1m$. We also define convergence to be the value of l where the exponential term is

10^{-6} of its value when $l = 0$. Plugging these values in we find we need $l = \frac{10^4 \ln 10^6}{0.1\pi} = 439761$ terms to achieve convergence.

Given that we in fact have a double sum to perform in equation (57) it is clear that there are severe computations issues with this approach. Although Ozkan and Raghavan¹⁸ do address many of these computational issues they do not satisfactorily address all of them, the main issue being their approximation for the long time behaviour of solutions like that in equation (57), which they admit is slow.

Appendix C Function Definitions

$$(60) \quad U(t - t_0) = \begin{cases} 1 & t > t_0 \\ 0 & t < t_0 \end{cases}$$

$$(61) \quad \text{erf}(x) = \frac{2}{\sqrt{\pi}} \int_0^x e^{-u^2} du$$

$$(62) \quad S_x(x, \tau) = \Theta_3 \left(\frac{\pi}{2a}(x - x_0), e^{-\left(\frac{\pi}{a}\right)^2 \eta_x \tau} \right) + \Theta_3 \left(\frac{\pi}{2a}(x + x_0), e^{-\left(\frac{\pi}{a}\right)^2 \eta_x \tau} \right)$$

$$(63) \quad S_y(y, \tau) = \Theta_3 \left(\frac{\pi}{2b}(y - y_0), e^{-\left(\frac{\pi}{b}\right)^2 \eta_y \tau} \right) + \Theta_3 \left(\frac{\pi}{2b}(y + y_0), e^{-\left(\frac{\pi}{b}\right)^2 \eta_y \tau} \right)$$

$$(64) \quad S_z(z, \tau) = \Theta_3 \left(\frac{\pi}{2d}(z - z_0), e^{-\left(\frac{\pi}{d}\right)^2 \eta_z \tau} \right) + \Theta_3 \left(\frac{\pi}{2d}(z + z_0), e^{-\left(\frac{\pi}{d}\right)^2 \eta_z \tau} \right)$$

$$(65) \quad S_z^{\int} (z_{01}, z_{02}, z, \tau) = \Theta_3^{\int} \left(\frac{\pi}{2d}(z - z_{01}), e^{-\left(\frac{\pi}{d}\right)^2 \eta_z \tau} \right) + \Theta_3^{\int} \left(\frac{\pi}{2d}(z + z_{02}), e^{-\left(\frac{\pi}{d}\right)^2 \eta_z \tau} \right) \\ - \Theta_3^{\int} \left(\frac{\pi}{2d}(z - z_{02}), e^{-\left(\frac{\pi}{d}\right)^2 \eta_z \tau} \right) - \Theta_3^{\int} \left(\frac{\pi}{2d}(z + z_{01}), e^{-\left(\frac{\pi}{d}\right)^2 \eta_z \tau} \right)$$

(66)

$$\begin{aligned}
S_x \iint (x_{01}, x_{02}, x_{03}, x_{04}, \tau) &= \Theta_3 \int_3 \left(\frac{\pi}{2a} (x_{04} - x_{01}), e^{-\left(\frac{\pi}{a}\right)^2 \eta_x \tau} \right) + \Theta_3 \int_3 \left(\frac{\pi}{2a} (x_{04} + x_{02}), e^{-\left(\frac{\pi}{a}\right)^2 \eta_x \tau} \right) \\
&- \Theta_3 \int_3 \left(\frac{\pi}{2a} (x_{04} - x_{02}), e^{-\left(\frac{\pi}{a}\right)^2 \eta_x \tau} \right) - \Theta_3 \int_3 \left(\frac{\pi}{2a} (x_{04} + x_{01}), e^{-\left(\frac{\pi}{a}\right)^2 \eta_x \tau} \right) \\
&- \Theta_3 \int_3 \left(\frac{\pi}{2a} (x_{03} - x_{01}), e^{-\left(\frac{\pi}{a}\right)^2 \eta_x \tau} \right) - \Theta_3 \int_3 \left(\frac{\pi}{2a} (x_{03} + x_{02}), e^{-\left(\frac{\pi}{a}\right)^2 \eta_x \tau} \right) \\
&+ \Theta_3 \int_3 \left(\frac{\pi}{2a} (x_{03} - x_{02}), e^{-\left(\frac{\pi}{a}\right)^2 \eta_x \tau} \right) + \Theta_3 \int_3 \left(\frac{\pi}{2a} (x_{03} + x_{01}), e^{-\left(\frac{\pi}{a}\right)^2 \eta_x \tau} \right)
\end{aligned}$$

(67)

$$\begin{aligned}
S_z \iint (z_{01}, z_{02}, z_{03}, z_{04}, \tau) &= \Theta_3 \int_3 \left(\frac{\pi}{2d} (z_{04} - z_{01}), e^{-\left(\frac{\pi}{d}\right)^2 \eta_z \tau} \right) + \Theta_3 \int_3 \left(\frac{\pi}{2d} (z_{04} + z_{02}), e^{-\left(\frac{\pi}{d}\right)^2 \eta_z \tau} \right) \\
&- \Theta_3 \int_3 \left(\frac{\pi}{2d} (z_{04} - z_{02}), e^{-\left(\frac{\pi}{d}\right)^2 \eta_z \tau} \right) - \Theta_3 \int_3 \left(\frac{\pi}{2d} (z_{04} + z_{01}), e^{-\left(\frac{\pi}{d}\right)^2 \eta_z \tau} \right) \\
&- \Theta_3 \int_3 \left(\frac{\pi}{2d} (z_{03} - z_{01}), e^{-\left(\frac{\pi}{d}\right)^2 \eta_z \tau} \right) - \Theta_3 \int_3 \left(\frac{\pi}{2d} (z_{03} + z_{02}), e^{-\left(\frac{\pi}{d}\right)^2 \eta_z \tau} \right) \\
&+ \Theta_3 \int_3 \left(\frac{\pi}{2d} (z_{03} - z_{02}), e^{-\left(\frac{\pi}{d}\right)^2 \eta_z \tau} \right) + \Theta_3 \int_3 \left(\frac{\pi}{2d} (z_{03} + z_{01}), e^{-\left(\frac{\pi}{d}\right)^2 \eta_z \tau} \right)
\end{aligned}$$

(68)

$$\begin{aligned}
B_x(x, y, z, \tau) &= \sum_{m=0}^{\infty} \sum_{l=0}^{\infty} \varepsilon_m \varepsilon_l \cos\left(\frac{m\pi y}{b}\right) \cos\left(\frac{l\pi z}{d}\right) e^{\left\{\left(\frac{m\pi}{b}\right)^2 \eta_y + \left(\frac{l\pi}{d}\right)^2 \eta_z\right\}(t-\tau)} \\
&\times \left\{ \overline{\overline{\psi}}_{0yz}(m, l, \tau) \Theta_3 \left(\frac{\pi x}{2a}, e^{-\left(\frac{\pi}{a}\right)^2 \eta_x (t-\tau)} \right) - \overline{\overline{\psi}}_{ayz}(m, l, \tau) \Theta_4 \left(\frac{\pi x}{2a}, e^{-\left(\frac{\pi}{a}\right)^2 \eta_x (t-\tau)} \right) \right\}
\end{aligned}$$

(69)

$$\begin{aligned}
B_y(x, y, z, \tau) &= \sum_{n=0}^{\infty} \sum_{l=0}^{\infty} \varepsilon_n \varepsilon_l \cos\left(\frac{n\pi x}{a}\right) \cos\left(\frac{l\pi z}{d}\right) e^{\left\{\left(\frac{n\pi}{a}\right)^2 \eta_x + \left(\frac{l\pi}{d}\right)^2 \eta_z\right\}(t-\tau)} \\
&\times \left\{ \overline{\overline{\psi}}_{x0z}(n, l, \tau) \Theta_3 \left(\frac{\pi y}{2b}, e^{-\left(\frac{\pi}{b}\right)^2 \eta_y (t-\tau)} \right) - \overline{\overline{\psi}}_{xbz}(n, l, \tau) \Theta_4 \left(\frac{\pi y}{2b}, e^{-\left(\frac{\pi}{b}\right)^2 \eta_y (t-\tau)} \right) \right\}
\end{aligned}$$

(70)

$$B_z(x, y, z, \tau) = \sum_{n=0}^{\infty} \sum_{m=0}^{\infty} \vartheta_n \vartheta_m \cos\left(\frac{n\pi x}{a}\right) \cos\left(\frac{m\pi y}{b}\right) e^{\left\{\left(\frac{n\pi}{a}\right)^2 \eta_x + \left(\frac{m\pi}{b}\right)^2 \eta_y\right\}(t-\tau)} \\ \times \left\{ \overline{\overline{\psi}}_{xy0}(n, m, \tau) \Theta_3\left(\frac{\pi z}{2d}, e^{-\left(\frac{\pi}{d}\right)^2 \eta_z(t-\tau)}\right) - \overline{\overline{\psi}}_{xyd}(n, m, \tau) \Theta_4\left(\frac{\pi z}{2d}, e^{-\left(\frac{\pi}{d}\right)^2 \eta_z(t-\tau)}\right) \right\}$$

(71)

$$B_x^{\int}(x, y, z_{01}, z_{02}, \tau) = \sum_{m=0}^{\infty} \sum_{l=0}^{\infty} \vartheta_m \vartheta_l \frac{d}{l\pi} \cos\left(\frac{m\pi y}{b}\right) \left[\sin\left(\frac{l\pi z_{02}}{d}\right) - \sin\left(\frac{l\pi z_{01}}{d}\right) \right] e^{\left\{\left(\frac{m\pi}{b}\right)^2 \eta_y + \left(\frac{l\pi}{d}\right)^2 \eta_z\right\}(t-\tau)} \\ \times \left\{ \overline{\overline{\psi}}_{0yz}(m, l, \tau) \Theta_3\left(\frac{\pi x}{2a}, e^{-\left(\frac{\pi}{a}\right)^2 \eta_x(t-\tau)}\right) - \overline{\overline{\psi}}_{ayz}(m, l, \tau) \Theta_4\left(\frac{\pi x}{2a}, e^{-\left(\frac{\pi}{a}\right)^2 \eta_x(t-\tau)}\right) \right\}$$

(72)

$$B_y^{\int}(x, y, z_{01}, z_{02}, \tau) = \sum_{n=0}^{\infty} \sum_{l=0}^{\infty} \vartheta_n \vartheta_l \frac{d}{l\pi} \cos\left(\frac{n\pi x}{a}\right) \left[\sin\left(\frac{l\pi z_{02}}{d}\right) - \sin\left(\frac{l\pi z_{01}}{d}\right) \right] e^{\left\{\left(\frac{n\pi}{a}\right)^2 \eta_x + \left(\frac{l\pi}{d}\right)^2 \eta_z\right\}(t-\tau)} \\ \times \left\{ \overline{\overline{\psi}}_{x0z}(n, l, \tau) \Theta_3\left(\frac{\pi y}{2b}, e^{-\left(\frac{\pi}{b}\right)^2 \eta_y(t-\tau)}\right) - \overline{\overline{\psi}}_{xbz}(n, l, \tau) \Theta_4\left(\frac{\pi y}{2b}, e^{-\left(\frac{\pi}{b}\right)^2 \eta_y(t-\tau)}\right) \right\}$$

(73)

$$B_z^{\int}(x, y, z_{01}, z_{02}, \tau) = \frac{2d}{\pi} \sum_{n=0}^{\infty} \sum_{m=0}^{\infty} \vartheta_n \vartheta_m \cos\left(\frac{n\pi x}{a}\right) \cos\left(\frac{m\pi y}{b}\right) e^{\left\{\left(\frac{n\pi}{a}\right)^2 \eta_x + \left(\frac{m\pi}{b}\right)^2 \eta_y\right\}(t-\tau)} \\ \times \left\{ \overline{\overline{\psi}}_{xy0}(n, m, \tau) \Theta_z^{\int}\left(\frac{\pi z}{2d}, e^{-\left(\frac{\pi}{d}\right)^2 \eta_z(t-\tau)}\right) - \overline{\overline{\psi}}_{xyd}(n, m, \tau) \Theta_z^{\int}\left(\frac{\pi z}{2d}, e^{-\left(\frac{\pi}{d}\right)^2 \eta_z(t-\tau)}\right) \right\}$$

$$(74) \quad I_x(u, x) = \Theta_3\left(\frac{\pi}{2a}(x-u), e^{-\left(\frac{\pi}{a}\right)^2 \eta_x t}\right) + \Theta_3\left(\frac{\pi}{2a}(x+u), e^{-\left(\frac{\pi}{a}\right)^2 \eta_x t}\right)$$

$$(75) \quad I_y(v, y) = \Theta_3\left(\frac{\pi}{2b}(y-v), e^{-\left(\frac{\pi}{b}\right)^2 \eta_y t}\right) + \Theta_3\left(\frac{\pi}{2b}(y+v), e^{-\left(\frac{\pi}{b}\right)^2 \eta_y t}\right)$$

$$(76) \quad I_z(w, z) = \Theta_3\left(\frac{\pi}{2d}(z-w), e^{-\left(\frac{\pi}{d}\right)^2 \eta_z t}\right) + \Theta_3\left(\frac{\pi}{2d}(z+w), e^{-\left(\frac{\pi}{d}\right)^2 \eta_z t}\right)$$

(77)

$$I_z^\int (w, z_{01}, z_{02}) = \Theta_3 \left(\frac{\pi}{2d} (z_{02} - w), e^{-\left(\frac{\pi}{d}\right)^2 \eta_{z,t}} \right) + \Theta_3 \left(\frac{\pi}{2d} (z_{02} + w), e^{-\left(\frac{\pi}{d}\right)^2 \eta_{z,t}} \right) \\ - \Theta_3 \left(\frac{\pi}{2d} (z_{01} - w), e^{-\left(\frac{\pi}{d}\right)^2 \eta_{z,t}} \right) - \Theta_3 \left(\frac{\pi}{2d} (z_{01} + w), e^{-\left(\frac{\pi}{d}\right)^2 \eta_{z,t}} \right)$$

$$(78) \quad \bar{\bar{\bar{\psi}}}_{0yz} (m, l, \tau) = \int_0^b \int_0^d \bar{\bar{\psi}}_{0yz} (y, z, \tau) \cos \left(\frac{l\pi z}{d} \right) \cos \left(\frac{m\pi y}{b} \right) dz dy$$

$$(79) \quad \bar{\bar{\bar{\psi}}}_{ayz} (m, l, \tau) = \int_0^b \int_0^d \bar{\bar{\psi}}_{ayz} (y, z, \tau) \cos \left(\frac{l\pi z}{d} \right) \cos \left(\frac{m\pi y}{b} \right) dz dy$$

$$(80) \quad \bar{\bar{\bar{\psi}}}_{x0z} (n, l, \tau) = \int_0^a \int_0^d \bar{\bar{\psi}}_{x0z} (x, z, \tau) \cos \left(\frac{l\pi z}{d} \right) \cos \left(\frac{n\pi x}{a} \right) dz dx$$

$$(81) \quad \bar{\bar{\bar{\psi}}}_{xbz} (n, l, \tau) = \int_0^a \int_0^d \bar{\bar{\psi}}_{xbz} (x, z, \tau) \cos \left(\frac{l\pi z}{d} \right) \cos \left(\frac{n\pi x}{a} \right) dz dx$$

$$(82) \quad \bar{\bar{\bar{\psi}}}_{xy0} (n, m, \tau) = \int_0^a \int_0^b \bar{\bar{\psi}}_{xy0} (x, y, \tau) \cos \left(\frac{m\pi y}{b} \right) \cos \left(\frac{n\pi x}{a} \right) dy dx$$

$$(83) \quad \bar{\bar{\bar{\psi}}}_{xyd} (n, m, \tau) = \int_0^a \int_0^b \bar{\bar{\psi}}_{xyd} (x, y, \tau) \cos \left(\frac{m\pi y}{b} \right) \cos \left(\frac{n\pi x}{a} \right) dy dx$$

$$(84) \quad \bar{\bar{\bar{\bar{\psi}}}}_{0yz} (m, l, s) = \int_0^b \int_0^d \int_0^\infty \bar{\bar{\psi}}_{0yz} (y, z, \tau) \cos \left(\frac{l\pi z}{d} \right) \cos \left(\frac{m\pi y}{b} \right) e^{-s\tau} d\tau dz dy$$

$$(85) \quad \bar{\bar{\bar{\bar{\psi}}}}_{ayz} (m, l, s) = \int_0^b \int_0^d \int_0^\infty \bar{\bar{\psi}}_{ayz} (y, z, \tau) \cos \left(\frac{l\pi z}{d} \right) \cos \left(\frac{m\pi y}{b} \right) e^{-s\tau} d\tau dz dy$$

$$(86) \quad \bar{\bar{\bar{\bar{\psi}}}}_{x0z} (n, l, s) = \int_0^a \int_0^d \int_0^\infty \bar{\bar{\psi}}_{x0z} (x, z, \tau) \cos \left(\frac{l\pi z}{d} \right) \cos \left(\frac{n\pi x}{a} \right) e^{-s\tau} d\tau dz dx$$

$$(87) \quad \bar{\bar{\bar{\bar{\psi}}}}_{xbz} (n, l, s) = \int_0^a \int_0^d \int_0^\infty \bar{\bar{\psi}}_{xbz} (x, z, \tau) \cos \left(\frac{l\pi z}{d} \right) \cos \left(\frac{n\pi x}{a} \right) e^{-s\tau} d\tau dz dx$$

$$(88) \quad \bar{\bar{\bar{\bar{\psi}}}}_{xy0} (n, m, s) = \int_0^a \int_0^b \int_0^\infty \bar{\bar{\psi}}_{xy0} (x, y, \tau) \cos \left(\frac{m\pi y}{b} \right) \cos \left(\frac{n\pi x}{a} \right) e^{-s\tau} d\tau dy dx$$

$$(89) \quad \bar{\bar{\bar{\psi}}}_{xyd}(n, m, s) = \int_0^a \int_0^b \int_0^\infty \psi_{xyd}(x, y, \tau) \cos\left(\frac{m\pi y}{b}\right) \cos\left(\frac{n\pi x}{a}\right) e^{-s\tau} d\tau dy dx$$

$$(90) \quad \bar{\bar{\bar{p}}}(n, m, l, s) = \int_0^a \int_0^b \int_0^d \int_0^\infty p(x, y, z, t) \cos\left(\frac{l\pi z}{d}\right) \cos\left(\frac{m\pi y}{b}\right) \cos\left(\frac{n\pi x}{a}\right) e^{-st} dt dz dy dx$$

Many of the analytical solutions we present in this paper use elliptical theta functions. We define the basic elliptical theta functions as in Abramowitz & Stegun²⁴, although the reader should be aware that there are alternative definitions e.g. Spanier & Oldham²⁵. Despite these functions consisting of infinite sums they converge very rapidly indeed for all parameter input ranges. Our definitions are as follows:

$$(91) \quad \theta_3(\pi x, e^{-\pi^2 t}) = \left. \begin{aligned} &1 + 2 \sum_{n=1}^{\infty} e^{-n^2 \pi^2 t} \cos(2n\pi x) \\ &\frac{1}{\sqrt{\pi t}} \sum_{n=-\infty}^{\infty} e^{-(x+n)^2/t} \end{aligned} \right\} \begin{aligned} &e^{-\pi^2 t} > \frac{1}{\pi} \\ &e^{-\pi^2 t} \leq \frac{1}{\pi} \end{aligned}$$

$$(92) \quad \theta_4(\pi x, e^{-\pi^2 t}) = \left. \begin{aligned} &1 + 2 \sum_{n=1}^{\infty} (-1)^n e^{-n^2 \pi^2 t} \cos(2n\pi x) \\ &\frac{1}{\sqrt{\pi t}} \sum_{n=-\infty}^{\infty} e^{-(x+0.5+n)^2/t} \end{aligned} \right\} \begin{aligned} &e^{-\pi^2 t} > \frac{1}{\pi} \\ &e^{-\pi^2 t} \leq \frac{1}{\pi} \end{aligned}$$

$$(93) \quad \theta_3 \int (\pi x, e^{-\pi^2 t}) = \int_0^x \theta_3(\pi x', e^{-\pi^2 t}) dx' \\ = \left. \begin{aligned} &x + \sum_{n=1}^{\infty} \frac{1}{n\pi} e^{-n^2 \pi^2 t} \sin(2n\pi x) \\ &\frac{1}{2} \sum_{n=-\infty}^{\infty} \left[\operatorname{erf}\left(\frac{x+n}{\sqrt{t}}\right) - \operatorname{erf}\left(\frac{n}{\sqrt{t}}\right) \right] \end{aligned} \right\} \begin{aligned} &e^{-\pi^2 t} > \frac{1}{\pi} \\ &e^{-\pi^2 t} \leq \frac{1}{\pi} \end{aligned}$$

$$(94) \quad \theta_4 \int (\pi x, e^{-\pi^2 t}) = \int_0^x \theta_4(\pi x', e^{-\pi^2 t}) dx' \\ = \left. \begin{aligned} &x + \sum_{n=1}^{\infty} \frac{1}{n\pi} (-1)^n e^{-n^2 \pi^2 t} \sin(2n\pi x) \\ &\frac{1}{2} \sum_{n=-\infty}^{\infty} \left[\operatorname{erf}\left(\frac{x+0.5+n}{\sqrt{t}}\right) - \operatorname{erf}\left(\frac{0.5+n}{\sqrt{t}}\right) \right] \end{aligned} \right\} \begin{aligned} &e^{-\pi^2 t} > \frac{1}{\pi} \\ &e^{-\pi^2 t} \leq \frac{1}{\pi} \end{aligned}$$

(95)

$$\begin{aligned}
 \theta_3 \int_0^x (\pi x, e^{-\pi^2 t}) &= \int_0^x \theta_3 \int_0^x (\pi x', e^{-\pi^2 t}) dx' \\
 &= \left. \begin{aligned}
 &\frac{x^2}{2} + \frac{1}{2} \sum_{n=1}^{\infty} \frac{1}{n^2 \pi^2} e^{-n^2 \pi^2 t} \cos(2n\pi x) \\
 &\frac{1}{2\sqrt{\pi}} \sum_{n=-\infty}^{\infty} \sqrt{\pi} (x+n) \operatorname{erf} \left(\frac{x+n}{\sqrt{t}} \right) + \sqrt{t} \left(e^{-(x+n)^2/t} - e^{-n^2/t} \right) - \operatorname{erf} \left(\frac{n}{\sqrt{t}} \right) n\sqrt{\pi}
 \end{aligned} \right\} \begin{aligned}
 &e^{-\pi^2 t} > \frac{1}{\pi} \\
 &e^{-\pi^2 t} \leq \frac{1}{\pi}
 \end{aligned}
 \end{aligned}$$